Journal of Computational Science & Engineering 20 (2015) 639-644

Available at http://www.asocse.org **ISSN 1710-4068**

Recent Advances in Elastico-mechanoluminescent Materials

Xing Xin, Juncheng Zhang*, Yunze Long, Yanjie Liu, Yong Wan*

College of Physics, Qingdao University, Qingdao 266071, China

Abstract: **Elastico-mechanoluminescence (EML), a type of mechanoluminescence (ML) induced by the application of mechanical energy on a solid, has attracted much attention due to the non-destructive, reliable and recoverable advantages in mechano-optical conversion. This article provides a review of the research related to EML. This review mainly summarizes the development, properties, mechanism and applications of EML materials. The potential applications of EML materials in stress sensor, visualization of stress distribution, lighting and display, as well as bio-image are highlighted. The challenge is finally identified.**

Keywords: Mechanoluminescence; Elastico-mechanoluminescence; Stress sensor; Visualizing stress distribution; Lighting and display; Bio-image

Received 29 June 2015, Revised 23 September 2015, Accepted 25 September 2015

*Corresponding Author: Juncheng Zhang, jc-zhang@qdu.edu.cn; Yong Wan, wanyong@qdu.edu.cn

1. Introduction

Luminescence occurs when phosphors are excited by electron beam, ultraviolet ray, X-ray, or chemical reaction. According to the difference of excitation energy, luminescence can be classified into cathodoluminescence, photoluminescence, electrolumi nescence, chemiluminescence, and so on. In recent years, mechanoluminescence (ML) excited by mechanical energy has attracted more and more attention due to the potential applications in stress sensor, imaging, display and biomedical fields [1].

ML materials emit light when a form of mechanical energy is applied. The mechanical energy can be produced by rub, cut, cleavage, shake, scratch, compression, crush and friction. ML are divided into tribo-ML and deformation ML. Tribo-ML mainly originates from the contact phenomenon of two dissimilar materials induced triboelectricity, tribochemical reaction, tribothermal generation. The deformation ML can be further divided into fracto-ML (FML), plastico-ML (PML) and elastico-ML (EML) [2-4]. FML is induced by fracture of solids. In 1605, Francis Bacon first reported the phenomenon of FML that a flash were watched when the sugar was scraped. According to a rough estimation, 50% of inorganic compounds and 30% of organic molecular solids have been found to show FML, such as sugar, molecular crystals, alkali halides, quartz and minerals [5]. However, little attention has been paid on the application of FML materials due to the destructive and unrepeatable disadvantages in the past decades. PML is produced during plastic deformation of solids. EML is produced during elastic deformation of solids. More interesting, the intensity of EML has linear relation with mechanical energy and can recover completely by ultraviolet (UV) radiation [6, 7]. Due to the advantages of non-destructive, reliable and recoverable in mechano-optical conversion, EML materials have shown the potential applications in a variety of fields including stress sensing, visualization of stress distribution, imaging and display, as well as bio-image. This review mainly focuses on the developed EML materials, mechanism and applications.

2. EML materials

At present, the EML materials with different luminescent colors have been synthesized. The color of the emitted light includes purple, blue, green, yellow, orange and red, such as ZnS: Mn^{2+} (yellow) [8], $SrAl_2O_4$: Eu^{2+} (green) [9], $Ca_2Al_2SiO_7$: Ce^{3+} (blue) [10], $SiAl_2O_4$: Ce, Ho^{2+} (purple) [11], $SrCaMgSi_2O_7$: Eu^{2+} (blue-green) [12] and (Ba,Ca)TiO_3: Pr^{3+} (red) [13]. However, the brightness of most of EML is too weak to realize the practical applications. Table 1 shows the EML materials with intense brightness, and their properties. Through setting and analyzing the preparation method and luminescence property of EML materials, it is possible to find appropriate methods to obtain EML materials which can meet the demands of practical application.

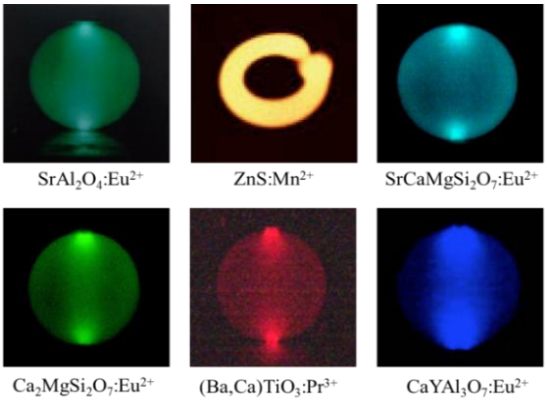

Figure 1. EML materials with different luminescentcolors [8, 14, 17, 19, 20, 21].

2.1. Preparation methods

Generally, solid state method is the most effective way to synthesize EML materials. All EML materials shown in Table 1 can be synthesized by the sold state

2015 © The American Computational Science Society. All rights reserved.

method. Take (Ba,Ca)TiO_3: Pr^{3+} for instance, the stoichiometric raw materials of $BaCO_3$, $CaCO_3$, TiO_2, Pr_6O_{11} (PrOOerialwere mixed thoroughly and prefired at 900 ℃ for 4 h, then remixed. The prefired powders were subsequently sintered at 1400 ℃ for 4 h to obtain (Ba,Ca)TiO_3: Pr^{3+} [13]. In addition, the other methods including sol-gel method [19], wet process [26], ion plating method [27], sputtering method [28] and hydrothermal method [29] have also been employed to prepare EML materials.

2.2. Brightness and wavelength of EML

The brightness of EML is one of the most important properties for EML materials. The ML with intense brightness could make the detection process simple and efficient. The luminescent color is also of importance for the different applications, such as lighting and display. Figure 1 shows the ML photographs of certain intense EML materials with different luminescent colors.

Table 1 Characteristics of certain EML materials [8,14-24]

No.	Materials	Report time	Synthesis method	Emission wavelength (nm)	Relation between ML intensity and load	Recoverability
1	$SrAl_2O_4:Eu^{2+}(Dy^{3+})$	1999	solid state	520 (green)	linear	UV-irradiation
2	$ZnS:Mn^{2+}$	1999	solid state	585 (yellow)	linear	UV-irradiation
3	ZrO_2:Ti	2002	solid state	480 (blue)	linear	UV-irradiation
4	$ZnAl_2O_4:Mn^{2+}$	2004	solid state	512 (green)	linear	UV-irradiation
5	$SrCaMgSi_2O_7:Eu^{2+}$	2007	solid state	493 (blue-greenish)	linear	UV-irradiation
6	$CaYAl_3O_7:Eu^{2+}$	2008	solid state	440 (blue)	linear	UV-irradiation
7	$Ca_2MgSi_2O_7:Eu^{2+},Dy^{2+}$	2009	solid state	530 (green)	linear	UV-irradiation
8	(Ba,Ca)$TiO_3:Pr^{3+}$	2010	solid state	613 (red)	linear	UV-irradiation
9	$CaYAl_3O_7:Ce^{3+}$	2011	solid state	421 (purple)	linear	UV-irradiation
10	$SrMg_2(PO_4)_2:Eu^{2+}$	2011	solid state	412 (purple)	linear	UV-irradiation
11	$CaZnOS:Mn^{2+}$	2013	solid state	610 (red)	linear	UV-irradiation
12	$CaZr(PO_4)_2:Eu^{2+}$	2013	solid state	472 (cyan)	linear	UV-irradiation
13	$Zn_2(Ge,Si)O_4:Mn^{2+}$	2015	solid state	542 (green)	linear	UV-irradiation

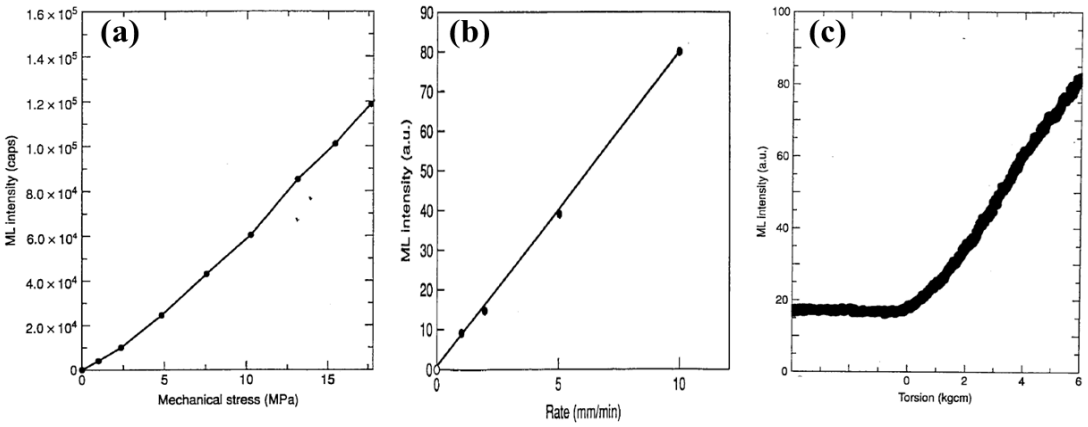

Figure 2. Different linear relation between EML intensity and mechanical parameters in $SrAl_2O_4:Eu^{2+}$. (a) EML intensity vs. stress; (b) EML intensity vs. deformation rate; (c) EML intensity vs. torsion [30].

2.3. Linear relation between EML and load

The characteristic of linear relation between EML intensity and mechanical parameter is the important basis for the practical application in visualization of stress distribution. Figure 2 shows the different linear relation between EML intensity and mechanical parameters in $SrAl_2O_4:Eu^{2+}$ [30]. It can be obviously observed that the EML intensity increases linearly with the increase of stress, deformation rate and torsion. Based on the linear relation, the stress distribution can be directly visualized from the difference of luminous on different parts and then further analyzed quantitatively by the distribution of EML intensity.

2.4. Recoverability

The recoverability of EML materials is the most

2015 © The American Computational Science Society. All rights reserved.

difference when compared with other kinds of ML materials. The recoverability mainly consists of two parts. One is the recoverability of shape and structure because of the elastic deformation, and another is the recoverability of EML intensity [13]. Figure 3(a) shows the EML decay phenomenon of (Ba, Ca) TiO_3: Pr^{3+} during reapplication of a compressive stress. In the first cycle, the EML intensity increased linearly with increasing compressive load, reaching a saturated peak value at the peak load, followed by sharp attenuation on releasing the compressive load. Although the EML intensity decayed significantly with stressed time in the later cycles, the EML intensity has the linear relation with the applied compressive load. However, the EML intensity can recover completely after UV irradiation, as shown in Figure 3(b). The same intense visible light emission is observed again. The damage on their samples is negligible after repetitive mechanical experiments. The nondestructive and recoverable EML is attractive for the practical applications of mechano-optical conversion.

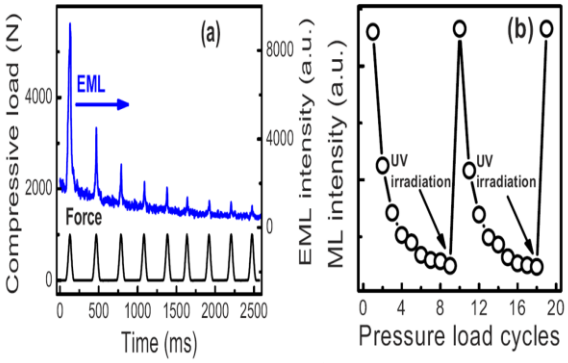

Figure 3. (a) EML decay behavior in (Ba,Ca)TiO_3:Pr^{3+} during the reapplication of load; (b) recoverability of EML in (Ba,Ca)TiO_3: Pr^{3+} [13].

3. EML mechanisms

It is generally believed that the process of EML and afterglow is similar, in which carriers (electron or hole) trapped at the trap levels are released effect by external circumstances and then recombines with the luminescence centers, resulting in photon emission. Temperature is the main influential factor for afterglow luminescence, while the dominating influential factor for EML is external force. Generally, the EML mechanisms is explained by the piezoelectrically induced trapped carrier de-trapping model, in which carriers (electron or hole) trapped at the trap levels are released under the piezoelectric field induced by mechanical stimulus and then recombines with the luminescence centers, resulting in photon emission [7].

3.1. EML mechanism of $SrAl_2O_4$:Eu^{2+}

At present, $SrAl_2O_4$: Eu^{2+} is one of the most promising EML materials due to the intense brightness and high sensitivity. Figure 4 illuminates the EML process in $SrAl_2O_4$: Eu^{2+}. In the carrier trap process, the electron of Eu^{2+} is excited to the conduction band under UV irradiation, leaving Eu^{3+}. When the excited electron is moving through the conduction band, it will be trapped at an oxygen defect. The trapped electron is considered to be stable at room temperature because the trap depth is estimated to be considerably higher than the thermal energy. When external force is applied, the trapped electron will be released to the conduction band. Then, it is recombined at the Eu^{3+} center and the inherent green light emission of Eu^{2+} can be observed [9].

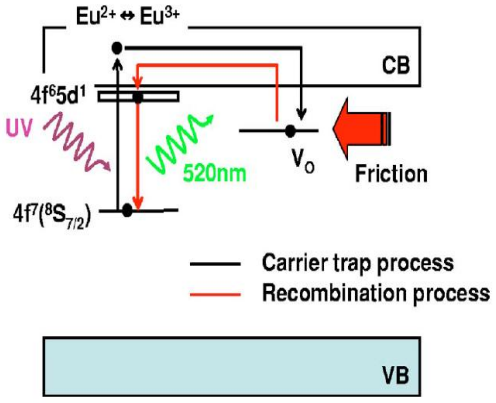

Figure 4. Schematic illumination of EML processes in $SrAl_2O_4$:Eu^{2+} [9].

3.2. EML mechanism of $CaZr(PO_4)_2$: Eu^{2+}

The EML mechanism of $CaZr(PO_4)_2$: Eu^{2+} is shown in Figure 5. While $CaZr(PO_4)_2$: Eu^{2+} is irradiated with UV light, the electrons are firstly excited from valence band to conduction band. Then the electrons will be trapped from the conduction band to an electron trap and migrate from one trap to another with the aid of acquiring (or releasing) thermal energy. When the external force is applied, a local electric field in the piezoelectric region will be formed due to the deformation of $CaZr(PO_4)_2$: Eu^{2+} lattice. When the external force is weak, electrons which located in the shallow trap levels could be excited to the conduction band. While the external force is strong, electrons in the deep trap levels could be excited to shallower contiguous trap levels, then to the conduction band, or directly to the conduction band by tunneling. The de-trapped electrons subsequently combined with luminescent center, and finally the cyan light emission will be observed [24].

4. Potential applications

4.1. Stress sensor

Traditional mechanical strain sensors need to have physical connection with the detected object while they are working, such as pressure sensor and piezoelectric sensor. These measurement methods are limited when the motion and deformation of the detected object have a drastic change. In comparison, the stress sensor based on the EML coatings have the

2015 © The American Computational Science Society. All rights reserved.

wireless and remote sensing advantages to detect different mechanical actions, including touch, impact, vibration, friction, stretching, compression [1]. It has a great potential application in detecting the deformation of dynamic object and irregular-shape body, such as engine, building, bridge and mechanical parts.

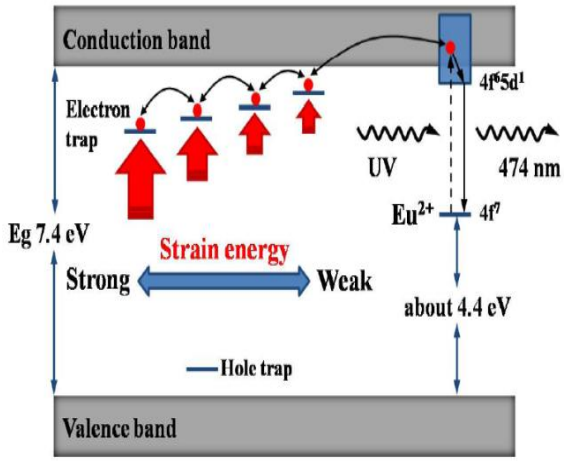

Figure 5. Schematic diagram of EML process for $CaZr(PO_4)_2$: Eu^{2+} [23].

4.2. Visualization of stress distribution

As abovementioned, the stress distribution can be directly observed from the distribution of EML intensity. Figure 6(a) demonstrates the signing habits of four signees based on an EML device composed of ZnS: Mn phosphors and PDMS [31]. The EML device can provide a high level of security to record of the signature graphics and the signing habits simultaneously. As shown in Figure 6(a), the first and second signee both intended to sign steadily with pressures evenly distributed through the whole signing process, while the first signee (Figure 6 a(i)) obviously signed with a stronger force than the second signee (Figure 6 a(ii)) did. The third signee (Figure 4 a(iii)) applied more pressures at the end of the signing process, and the forth signee (Figure 6 a(iv)) preferred signing with more pressures both at the end and some turning points of the signing process. Therefore, both the handwritten signatures and the signing habits of signees are recorded by the EML device.

4.3. Lighting and display

ML phosphors can be used to produce wind-driven light sources and display devices. For example, a patterned ML device composed of PDMS elastomer and ZnS phosphors has been reported by Jeong and co-workers [32]. By controlling the mass ratio of PDMS elastomer and ZnS: Mn phosphors, they demonstrated light emission of tunable colors (including blue, green, red and white lights) following excitation by an air flow. Figure 6(b) presents the photograph of the patterned wind-driven ML. When the wind flows over a specific region, the rods in that region emit EML light due to the application of stress primarily to the connecting region between the rod and the base plate. Brighter EML could be observed near the rod-plate joint because the stress is primarily concentrated at the point where the rod bends. At the current stage of development, the wind-driven ML structure could be potentially used as natural wind-driven ML display or lighting system, such as a large-scale outdoor ML billboard with large pixels.

4.4. Bio-image

EML materials also possess a promising application in bio-image. It is well known that the ultrasound technology has been widely used in biomedical field. However it's hard to determine the vibration distribution when ultrasound arrived at body. With the development of EML materials with intense brightness and high sensitivity, the distribution of ultrasound can be determined by the detection of EML intensity with the aim of EML materials. Terasaki and co-workers demonstrated light emission from in-body EML materials stimulated by the out-body ultrasonic wave (Figure 6(c)) [33, 34]. The EML materials can also be used to monitor human activities by making into artificial organs or tissues, such as bone, tendon and arteries. The existing monitoring technology need to have a connection between body and electronic equipment with prolonged supply energy. It's well known that our body can provide sufficient mechanical energy from human activities continuously, such as running, muscle contractions, vasoconstriction. The human activities could be derived by monitoring the EML intensity of artificial organs or tissues [24].

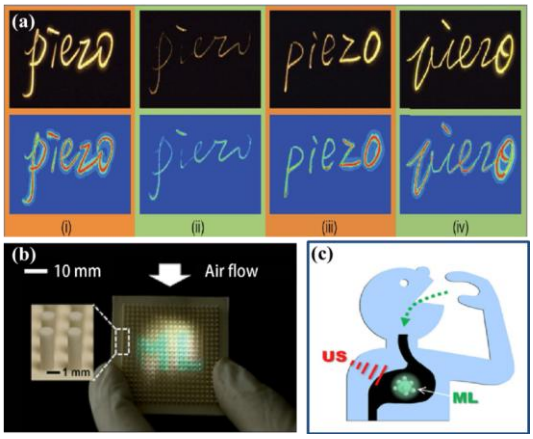

Figure 6. (a) Stress distribution of four signees. (b) Patterned ML device for a wind-driven display. (c) Schematic illustration of using ML phosphors for bio-imaging and phototherapy [32-34].

5. Challenges

5.1. Materials

At present, dozens of EML materials have been synthesized. Among them, some EML materials, such

2015 © The American Computational Science Society. All rights reserved.

as ZnS: Mn^{2+} (yellow) [8] and $SrAl_2O_4$: Eu^{2+} (green) [14] can emit visible emission light when they are excited with a variety of mechanical energy. However, the intensity of most EML materials is too weak to meet the requirements of practical application. On the one hand, the brightness of the developed EML phosphors needs to be further improved. On the other hand, it is necessary to exploit novel EML materials with high performance. Furthermore, the solid state method is the most common and effective method to produce EML materials. However, the micro-scale of EML particles is generally synthesized by solid state method. The size of particles is too large for the application in body. The high calcination temperature also consumes a lot of energy. Therefore, new synthesis methods should be considered to prepare EML materials according to the different requirements. The methods of characterizing ML phosphors should be standardized in the near future.

5.2. EML mechanisms

Up to now, there was no clear explanation for EML mechanisms due to the short research on EML and the limited EML materials. The research on EML materials is lack of in-depth and quantitative analysis. The explanation on EML mechanism is still limited to the superficial discussion of EML phenomenon. Many details concerning EML, such as the origin of the traps or the transfer pathway from traps to luminescent centers, remain unclear. The dynamic description on EML process is ambiguous so far. Further investigation is needed to understand the complete theory.

5.3. Applications

For the purpose of application, the standardization on the test procedures needs to be established. For the application in lighting and display (Figure 6(b)), the wind speed belongs to the range of hurricane or typhoon. Further improvement is needed to achieve bright ML under gentle breezes (a few meters per second). For the application in bio-issues, the biological compatibility should also be considered.

6. Conclusions

EML materials have attracted much attention due to the non-destructive, reliable and recoverable advantages in mechano-optical conversion. Dozens of EML materials have been synthesized in recent years. This review provides a summary on the development of EML materials, properties, mechanism and applications. The potential applications in stress sensor, visualization of stress distribution, lighting and display, as well as bio-image have been highlighted. Finally, the challenges have been discussed from three aspects including materials, mechanisms and applications. With the in-depth development of EML, we believe that EML materials will be utilized widely and effectively in most fields.

References:

[1] M. Saleem, R. Neema, M. Mittal, P.K. Sharma, Int. J. Sci. Res. in Physics and Applied Sciences, 3 (2015) 2348–3423.

[2] L.M. Sweeting, Chem. Mater., 13 (2001) 854-870.

[3] N.P. Bergeron, W.A. Hollerman, S.M. Goedeke, M. Hovater, W. Hubbs, A. Finchum, R.J. Moore, S.W. Allison, D.L. Edwards, Int J Impact Eng., 33 (2006) 91-99.

[4] B. P. Chandra, A.S. Rathore, Cryst. Res. Technol., 30 (1995) 885–896.

[5] C. N. Xu, W. Tadahiko, A. Morito, X.G Zheng, Appl. Phys. Lett., 74 (1999) 2414-2416.

[6] J.C. Zhang, C.N. Xu, Y.Z. Long, Opt. Express, 21 (2013) 13699-13709.

[7] S. Kamimura, H. Yamada, C.N. Xu, Appl. Phys. Lett., 101 (2012) 91113-91113-4.

[8] C.N. Xu, T. Watanabe, M. Akiyama, X.G. Zheng, Appl. Phys. Lett., 74 (1999) 1236-1238.

[9] Y. Hiroshi, X.Y. Fu, C.N. Xu, J. Electrochem. Soc., 154 (2007) 348-351.

[10] A. Morito, C.N. Xu, M. Hiroaki, N. Kazuhiro, W. Tadahiko, Appl. Phys. Lett., 75 (1999) 2548-2550.

[11] H.W. Zhang, Y. Hiroshi, T. Nao, C.N. Xu, Appl. Phys. Lett., 91 (2007) 081905- 081905-3.

[12] H.W. Zhang, H. Yamada, N. Terasakia , C.N. Xu, Electrochem. Solid-State Lett., 10 (2007) 129-131.

[13] J.C. Zhanga, X.S. Wang, X. Yao, C.N. Xu, H. Yamada, J. Electrochem. Soc., 157 (2010) 269-273.

[14] A. Morito, C.N. Xu, N. Kazuhiro, W. Tadahiko, Appl. Phys. Lett., 73(1998) 3046-3048.

[15] A. Morito, C.N. Xu, N. Kazuhiro, Appl. Phys. Lett., 81 (2002) 457-459.

[16] H. Matsui, C.N. Xu, Y. Liu, H. Tateyama, Phys. Rev. B, 69 (2004) 235107-235109.

[17] H.W. Zhang, H. Yamada, N. Terasaki, C.N. Xu, Electrochem. Solid-State Lett., 10 (2007) 129-131.

[18] H.W. Zhang, H. Yamada, N. Terasaki, C.N. Xu, J. Electrochem. Soc. 155(2008) 128-131.

[19] H.W. Zhang, N. Terasaki, H.Yamada, C.N. Xu, Thin Solid Films, 518 (2009) 610-613.

[20] J.C. Zhang, X.S. Wang, X. Yao, C.N. Xu, H. Yamada, J. Electrochem. Soc., 157 (2010) 269-273.

[21] H.W. Zhang, C.N. Xu, N. Terasaki, H. Yamada, Electrochem. Solid-State Lett., 14 (2011) 76-80.

[22] S. Kamimura, H. Yamada, C.N. Xu, J. Lumin., 132 (2011) 526-530.

[23] J.C. Zhang, C.N. Xu, S. Kamimura, Y. Terasawa, H. Yamada, X.S. Wang, Opt. Express, 21 (2013) 12976-12986.

[24] J.C. Zhang, C.N. Xu, Y.Z. Long, Opt. Express, 21 (2013) 13699-13709.

[25] H.F. Zhao, X.S. Wang, J. Li, Y.X. Li, X. Yao, Appl. Phys. Express, 9 (2016) 12104-3.

2015 © The American Computational Science Society. All rights reserved.

[26] T. Toriyi, Y. Adachi, H. Yamada, Y. Imai, C.N. Xu, Key Eng. Mater, 388 (2008) 301-304.
[27] C.N. Xu, T. Watanabe1, M. Akiyama1, X.G. Zheng, Mater. Res. Bull, 34 (1999) 1491-1500.
[28] X.Y. Fua, H.W. Zhang, L.J. Fang, H.X. Fu, Thin Solid Films, 540 (2013) 41-45.
[29] K.K. Satapathy, G.C. Mishra, F. Khan, Luminescence, 30 (2014) 564-567.
[30] C.N. Xu, Encyclopedia of smart materials, 2002.
[31] X.D. Wang, H.L. Zhang, R.M. Yu, L. Dong, D.F. Peng, A.H. Zhang, Y. Zhang, H. Liu, C.F. Pan, Z.L. Wang, Adv. Mater.. 27 (2015) 2324–2331.
[32] S.M. Jeong, S. Song, K. Joo, J. Kim, S. Hwang, J. Jeong, H. Kim, Energy Environ. Sci., 7 (2014) 3338–3346.
[33] N. Terasakia, H. Yamada, C.N. Xu, Catal. Today, 201 (2012) 203-208.
[34] N. Terasaki , H.W. Zhang, H. Yamada, C.N. Xu, Chem. Commun, 47 (2011) 8034-8036.

2015 © The American Computational Science Society. All rights reserved.